Forward Physics in ATLAS

Maciej Trzebiński

Institute of Nuclear Physics
Polish Academy of Sciences
Kraków, Poland

XXXI Cracow Epiphany Conference on the recent LHC Results

Kraków, Poland 16th January 2025

Usual proton-proton collisions at the LHC

→ protons collide head-on

→ both protons break up

→ collision products are emitted in the central region

→ proton remnants may be found in the forward regions

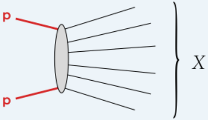

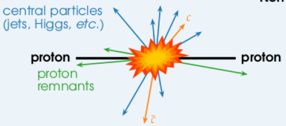

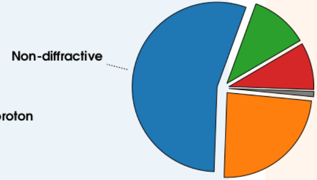

Collisions at LHC

Collisions at LHC

Usual proton-proton collisions at the LHC

- → protons collide head-on
- → both protons break up
- → collision products are emitted in the central region
- → proton remnants may be found in the forward regions

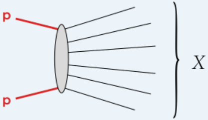

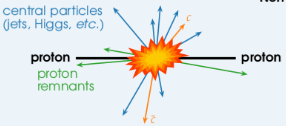

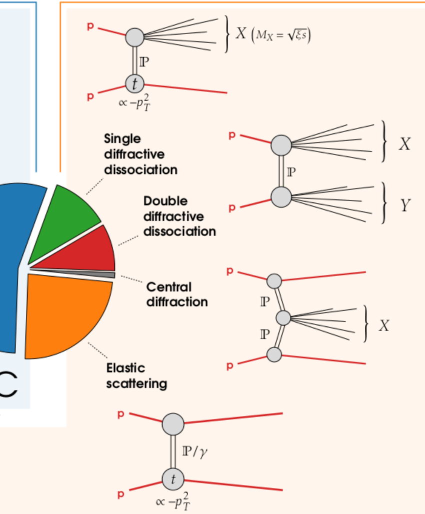

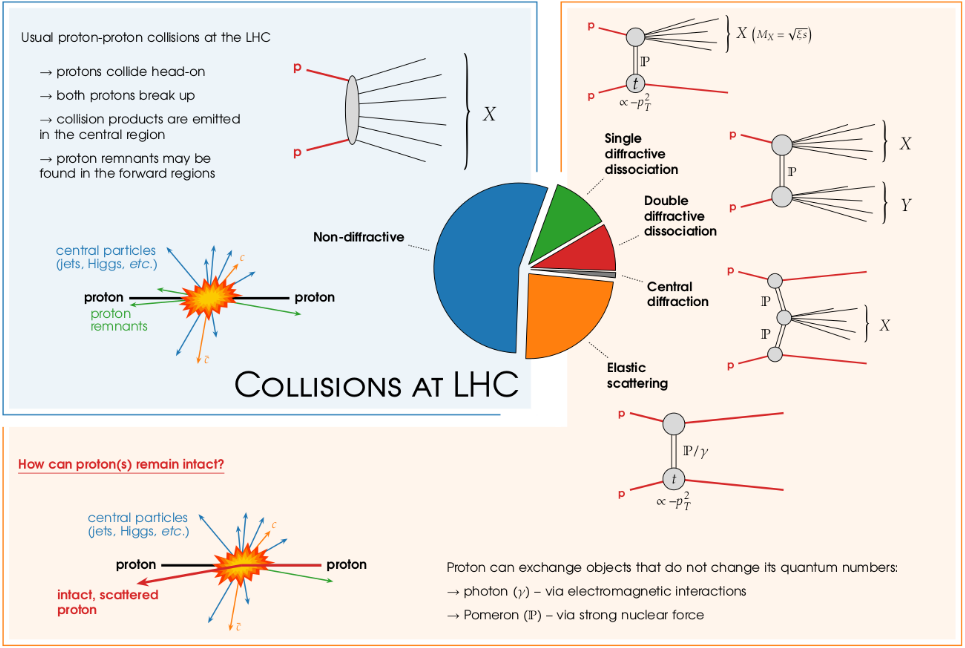

Usual proton-proton collisions at the LHC
→ protons collide head-on
→ both protons break up
→ collision products are emitted in the central region
→ proton remnants may be found in the forward regions
p
p
X
central particles (jets, Higgs, etc.)
proton
proton
proton remnants
c
c̄
Non-diffractive
Single diffractive dissociation
Double diffractive dissociation
Central diffraction
Elastic scattering
COLLISIONS AT LHC
X ($M_X = \sqrt{\xi s}$)
ℙ
t
$\propto -p_T^2$
X
Y
ℙ/γ
How can proton(s) remain intact?
central particles (jets, Higgs, etc.)
proton
proton
intact, scattered proton
Proton can exchange objects that do not change its quantum numbers:
→ photon (γ) – via electromagnetic interactions
→ Pomeron (ℙ) – via strong nuclear force

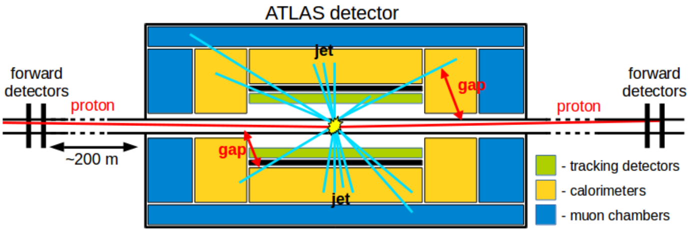

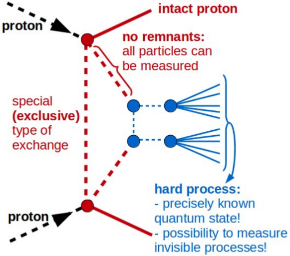

- Characteristic topology: presence of rapidity gap between the proton(s) and the "central" system;

Measuring rapidity gap:

+ "classically" used for diffractive pattern identification
+ no need for additional detectors
– gap is frequently destroyed due to pile-up background
– gap may be out of acceptance of "central" detector

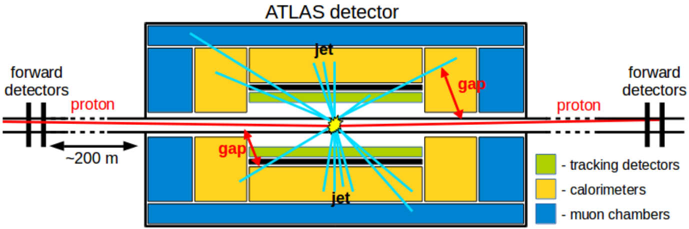

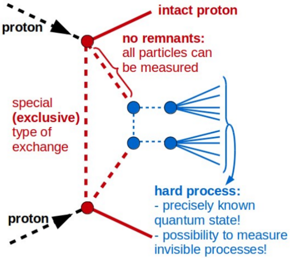

- Characteristic topology: presence of rapidity gap between the proton(s) and the "central" system; one or both interacting proton(s) remain intact.
- Intact protons scattered at very small angles → very close to the beam after the interaction → detectors must be located far from the Interaction Point (IP) → LHC magnetic fields (**optics**) must be considered.

Measuring rapidity gap:

\+ "classically" used for diffractive pattern identification
\+ no need for additional detectors
– gap is frequently destroyed due to pile-up background
– gap may be out of acceptance of "central" detector

Measuring forward protons:

\+ protons measured directly
\+ suitable for pile-up environment
– protons are scattered at very small angles
– additional detectors required far downstream

Intact protons → natural diffractive signature → usually scattered at very small angles (μrad) → detectors must be located far from the Interaction Point.

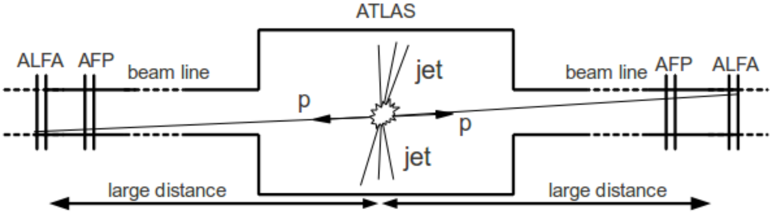

ALFA

- **A**bsolute **L**uminosity **F**or **A**TLAS
- 240 m from ATLAS IP
- soft diffraction (elastic scattering)
- special runs (high β^* optics)
- vertically inserted Roman Pots
- tracking detectors, resolution: $\sigma_x = \sigma_y = 30\ \mu$m
- in operation between 2011 and 2023

AFP

- **A**TLAS **F**orward **P**roton
- 210 m from ATLAS IP
- hard diffraction, BSM searches
- nominal runs (collision optics)
- horizontally inserted Roman Pots
- tracking detectors, resolution: $\sigma_{x/y} = 6/30\ \mu$m
- timing detectors, resolution: $\sigma_t \sim 25$ ps
- in operation since 2016 (one side) / 2017 (full set)

Roman Pot Technology (example of AFP)

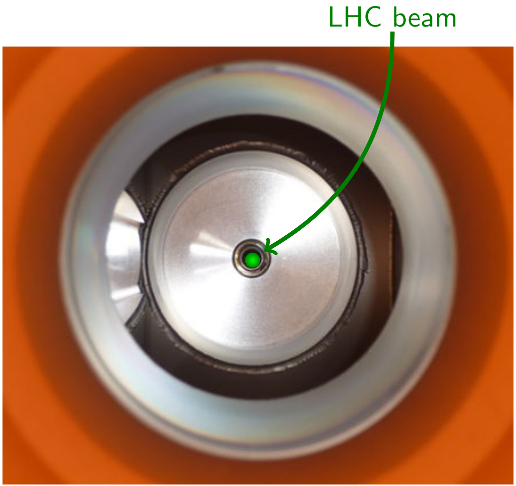
LHC beam

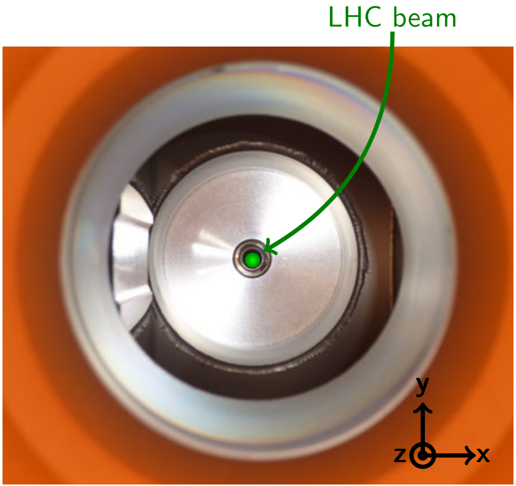
LHC beam
y
z
x

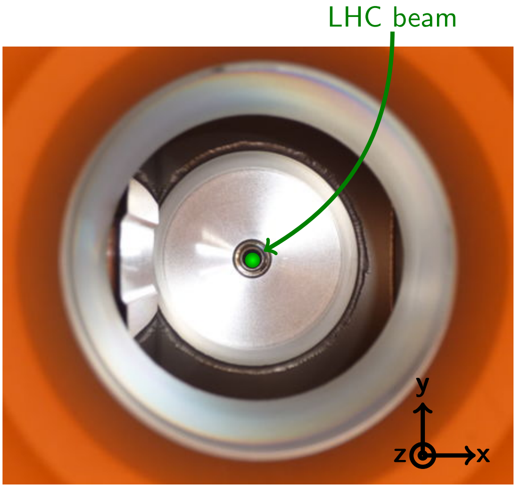
LHC beam
y
z
x

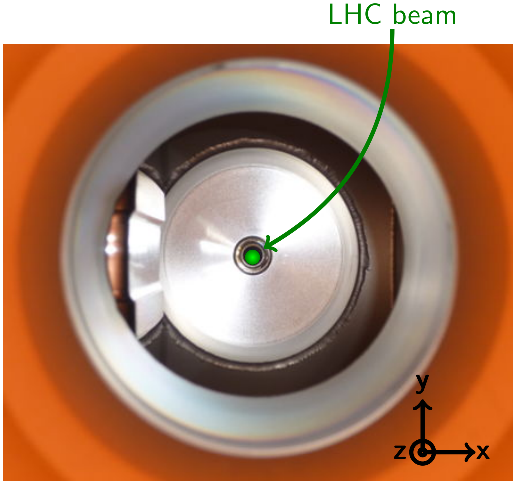
LHC beam
y
z
x

Roman Pot Technology (example of AFP)

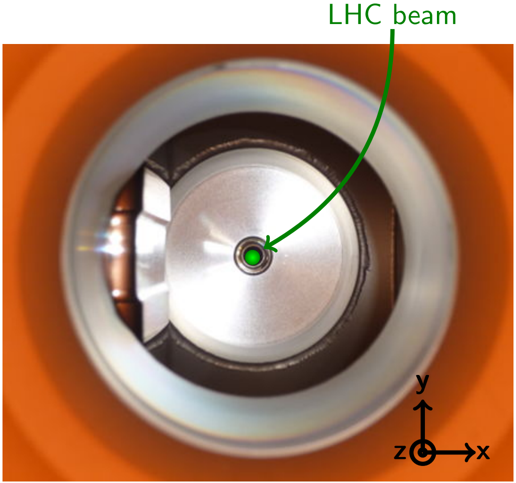

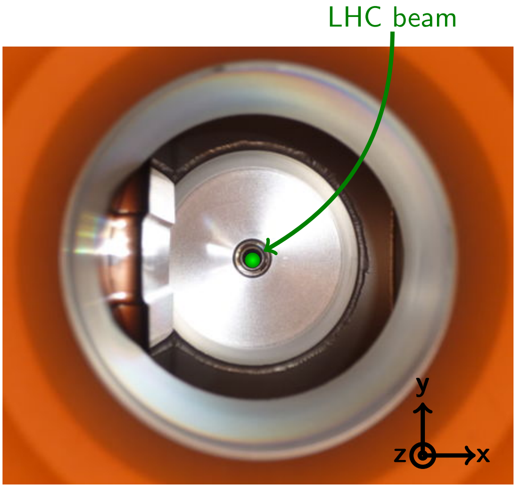
LHC beam
y
z
x

Roman Pot Technology (example of AFP)

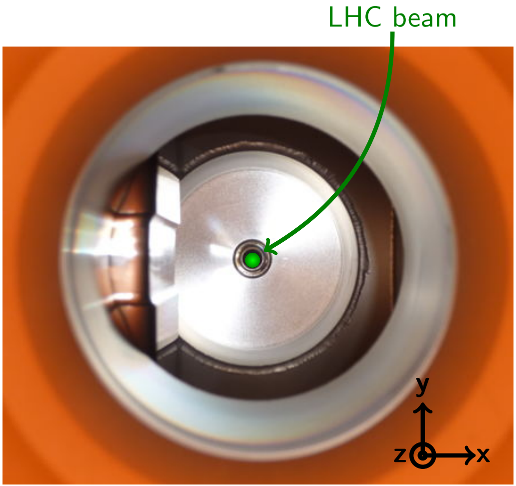

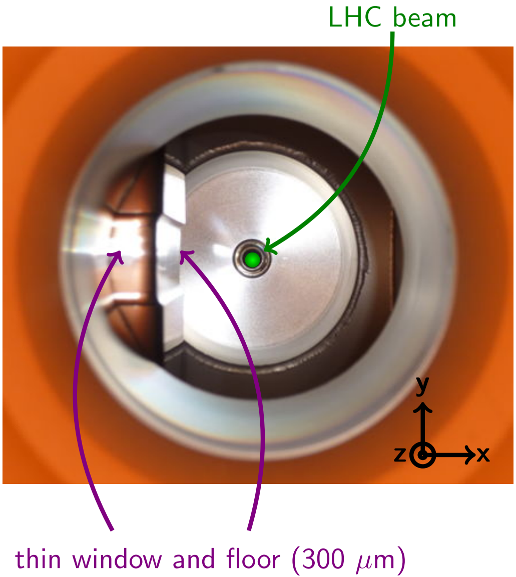
LHC beam
y
z
x
thin window and floor (300 μm)

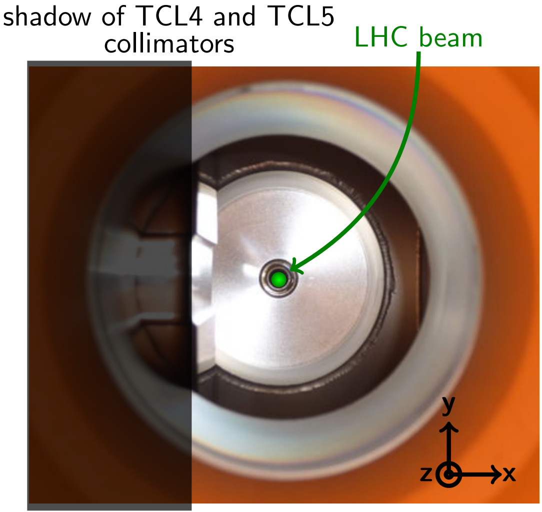

thin window and floor (300 μm)

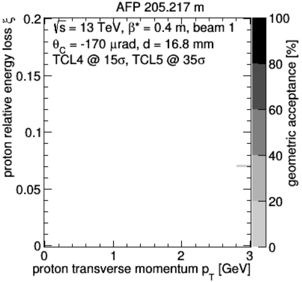

Geometric acceptance:

ratio of protons with a given $(\xi,\ p_T)$ that reached the detector to the total number of the scattered protons having given $(\xi,\ p_T)$

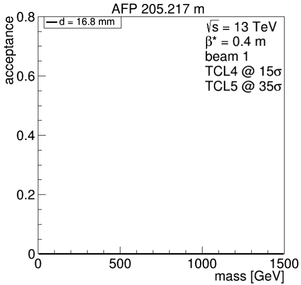

Mass acceptance:

mass of central system when both protons are tagged in Roman pot

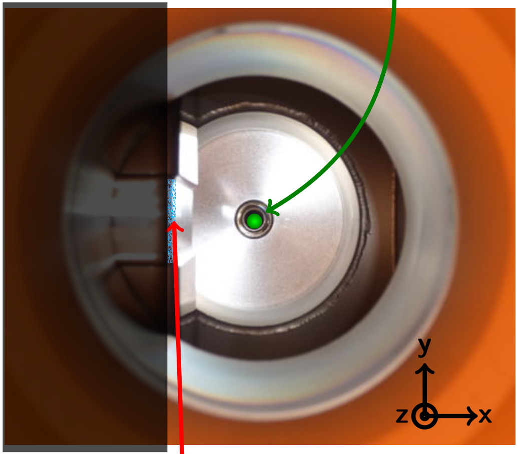

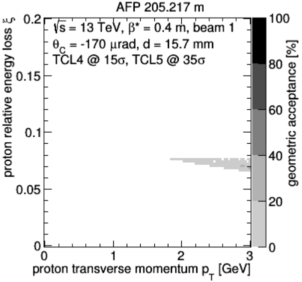

Geometric acceptance: ratio of protons with a given (ξ, p_T) that reached the detector to the total number of the scattered protons having given (ξ, p_T)

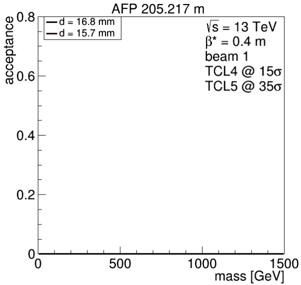

Mass acceptance: mass of central system when both protons are tagged in Roman pot

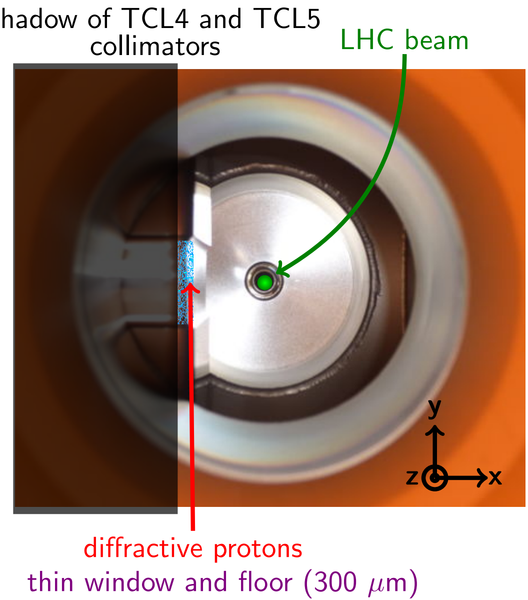

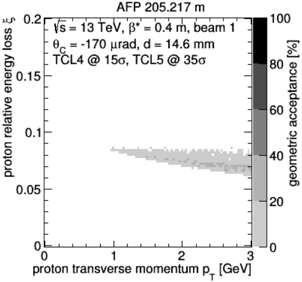

Geometric acceptance:

ratio of protons with a given $(\xi,\ p_T)$ that reached the detector to the total number of the scattered protons having given $(\xi,\ p_T)$

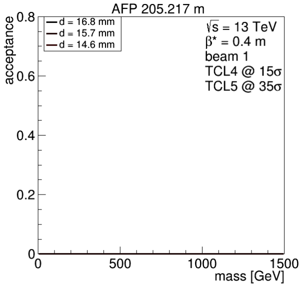

Mass acceptance:

mass of central system when both protons are tagged in Roman pot

shadow of TCL4 and TCL5 collimators

LHC beam

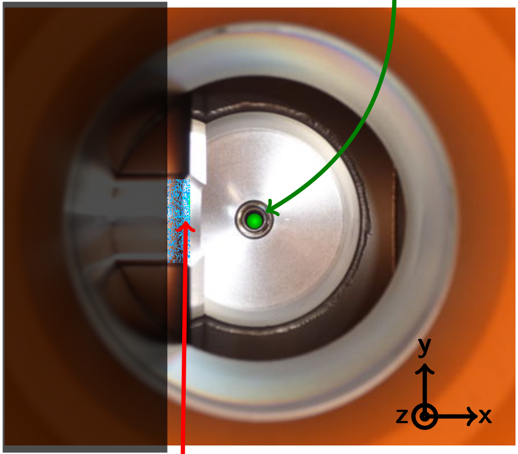

diffractive protons

thin window and floor (300 μm)

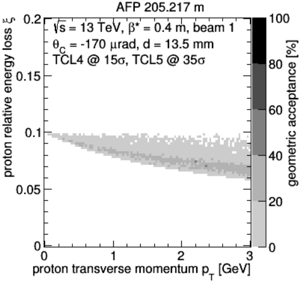

Geometric acceptance:

ratio of protons with a given (ξ, p_T) that reached the detector to the total number of the scattered protons having given (ξ, p_T)

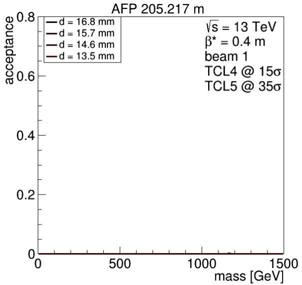

Mass acceptance:

mass of central system when both protons are tagged in Roman pot

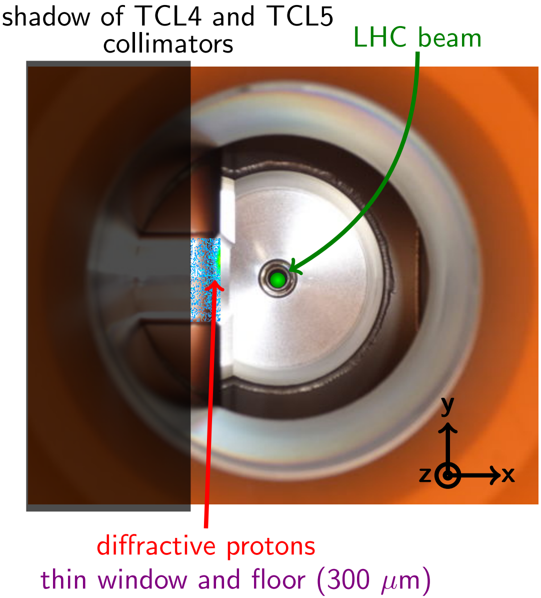

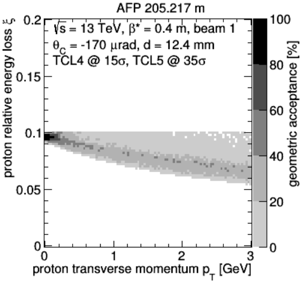

Geometric acceptance:

ratio of protons with a given $(\xi,\ p_T)$ that reached the detector to the total number of the scattered protons having given $(\xi,\ p_T)$

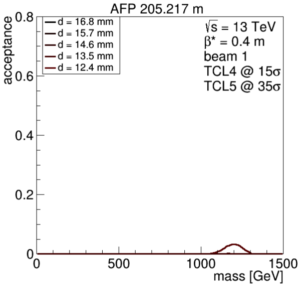

Mass acceptance:

mass of central system when both protons are tagged in Roman pot

shadow of TCL4 and TCL5 collimators

LHC beam

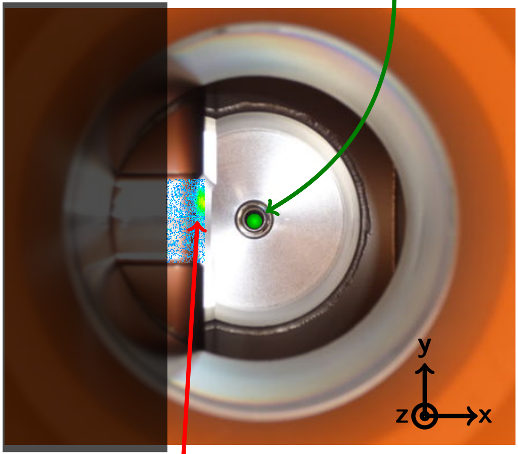

diffractive protons

thin window and floor (300 μm)

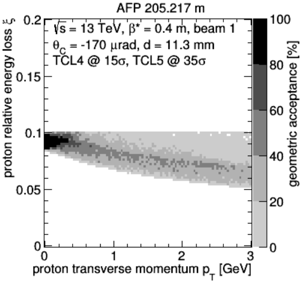

Geometric acceptance:

ratio of protons with a given $(\xi,\ p_T)$ that reached the detector to the total number of the scattered protons having given $(\xi,\ p_T)$

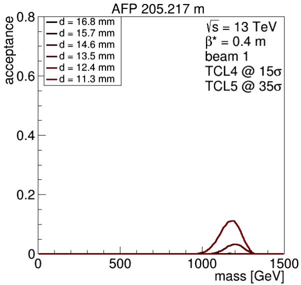

Mass acceptance:

mass of central system when both protons are tagged in Roman pot

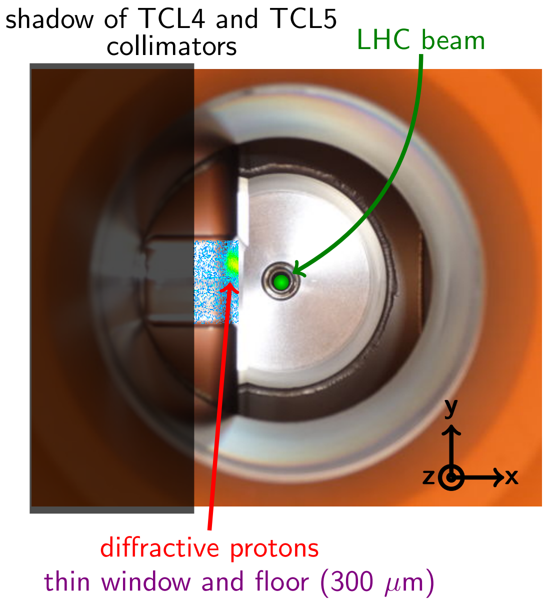

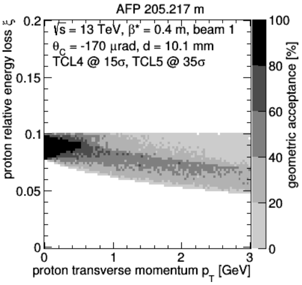

Geometric acceptance:

ratio of protons with a given $(\xi,\ p_T)$ that reached the detector to the total number of the scattered protons having given $(\xi,\ p_T)$

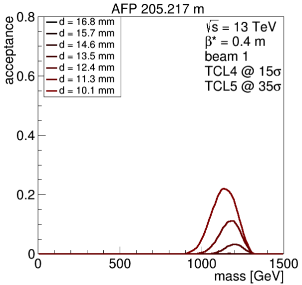

Mass acceptance:

mass of central system when both protons are tagged in Roman pot

shadow of TCL4 and TCL5 collimators

LHC beam

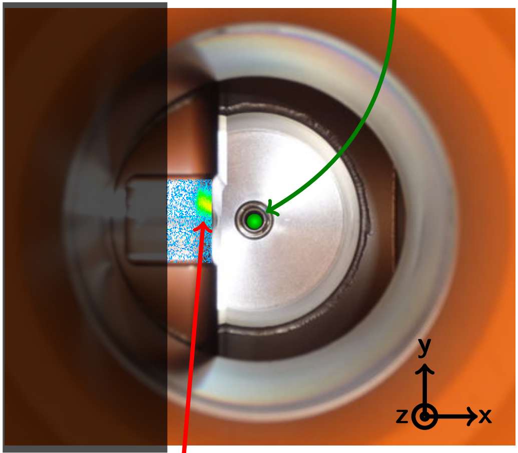

diffractive protons

thin window and floor (300 μm)

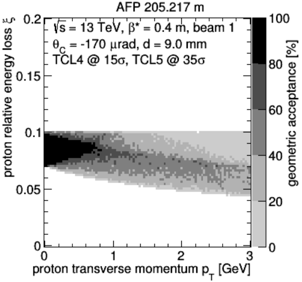

Geometric acceptance:

ratio of protons with a given $(\xi,\ p_T)$ that reached the detector to the total number of the scattered protons having given $(\xi,\ p_T)$

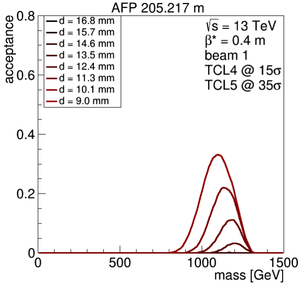

Mass acceptance:

mass of central system when both protons are tagged in Roman pot

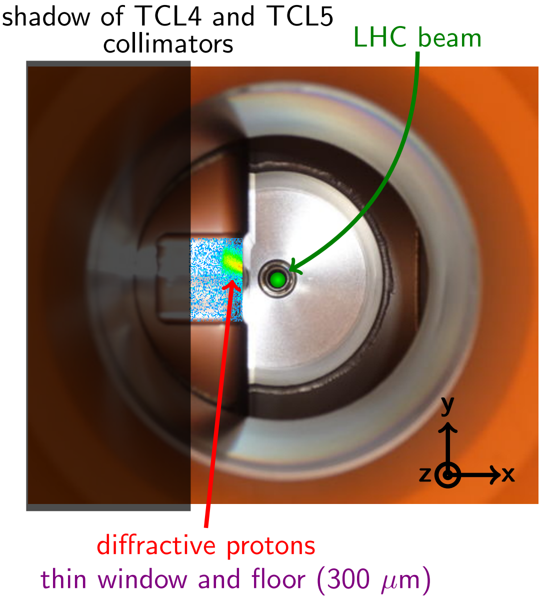

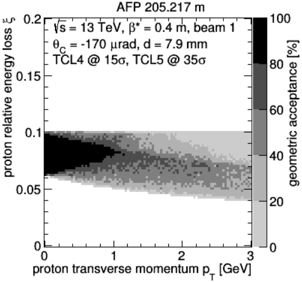

Geometric acceptance:

ratio of protons with a given $(\xi, \ p_T)$ that reached the detector to the total number of the scattered protons having given $(\xi, \ p_T)$

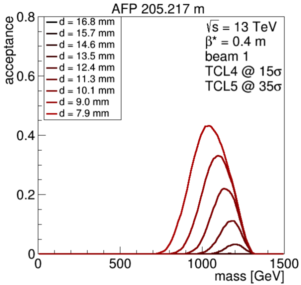

Mass acceptance:

mass of central system when both protons are tagged in Roman pot

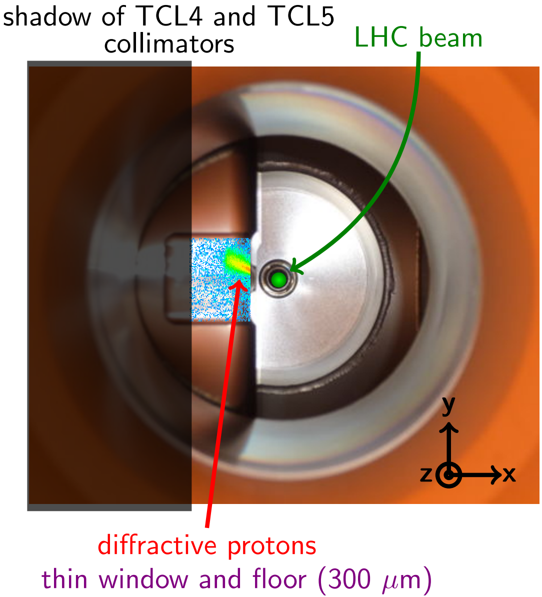

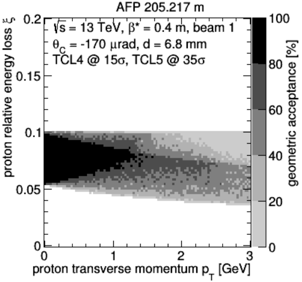

Geometric acceptance:
ratio of protons with a given $(\xi,\ p_T)$ that reached the detector to the total number of the scattered protons having given $(\xi,\ p_T)$

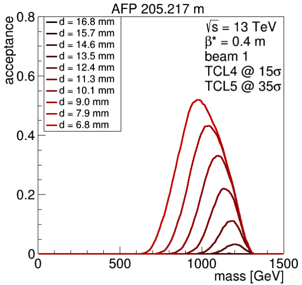

Mass acceptance:
mass of central system when both protons are tagged in Roman pot

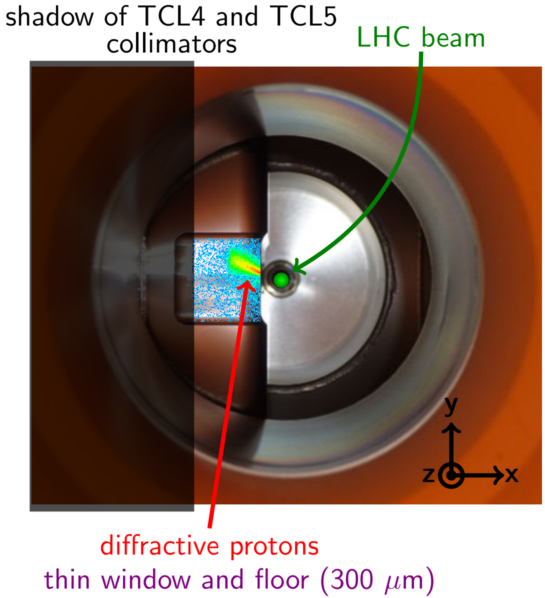

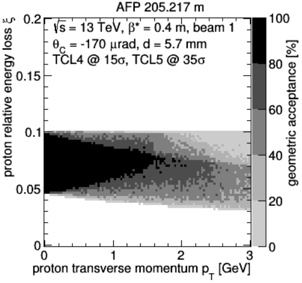

Geometric acceptance:

ratio of protons with a given $(\xi,\ p_T)$ that reached the detector to the total number of the scattered protons having given $(\xi,\ p_T)$

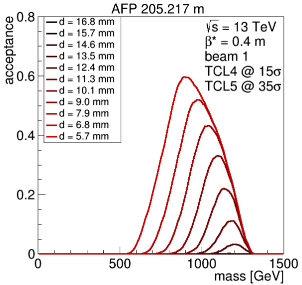

Mass acceptance:

mass of central system when both protons are tagged in Roman pot

shadow of TCL4 and TCL5 collimators

LHC beam

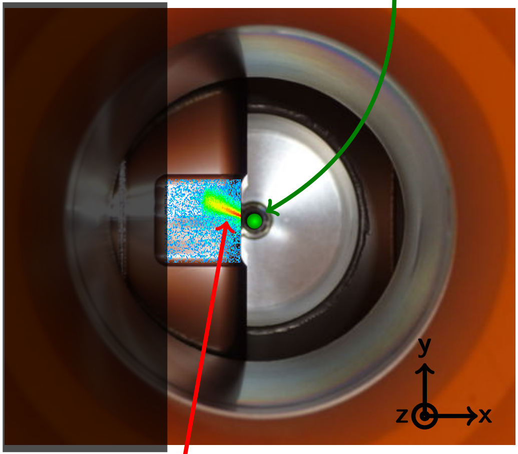

diffractive protons

thin window and floor (300 μm)

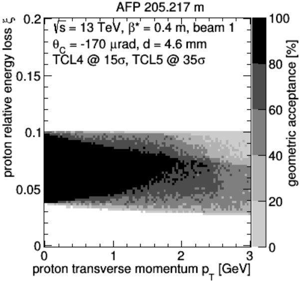

Geometric acceptance:

ratio of protons with a given (ξ, p_T) that reached the detector to the total number of the scattered protons having given (ξ, p_T)

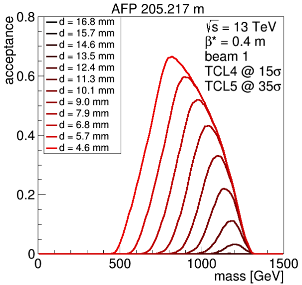

Mass acceptance:

mass of central system when both protons are tagged in Roman pot

shadow of TCL4 and TCL5 collimators

LHC beam

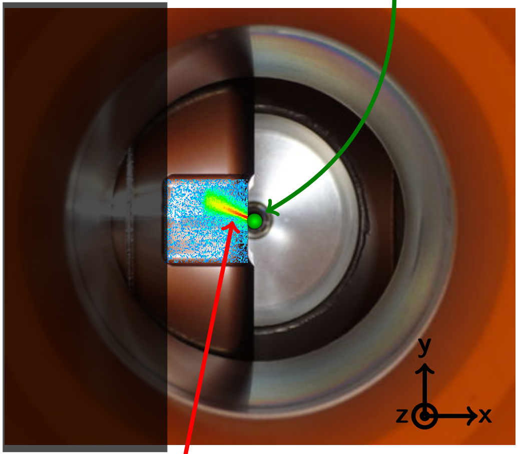

diffractive protons

thin window and floor (300 μm)

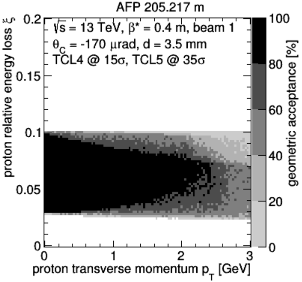

Geometric acceptance:

ratio of protons with a given (ξ, p_T) that reached the detector to the total number of the scattered protons having given (ξ, p_T)

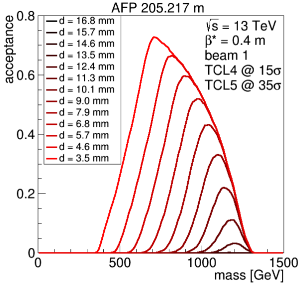

Mass acceptance:

mass of central system when both protons are tagged in Roman pot

"Usual" conditions: β^* in range 0.3 – 1.2 m $\rightarrow$ strongly focused beam (high pile-up):

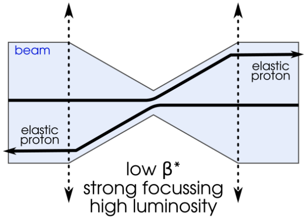

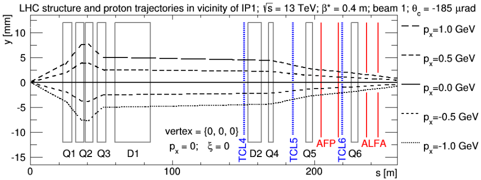

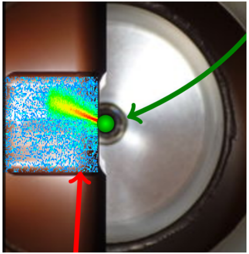

Special optics: β^* of 90 m, 120 m, 2.5 km, 3/6 km $\rightarrow$ weak, parallel-to-point focusing (low pile-up):

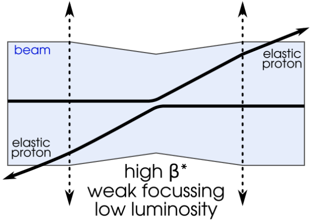

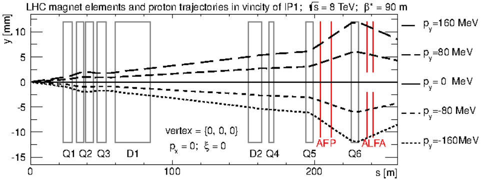

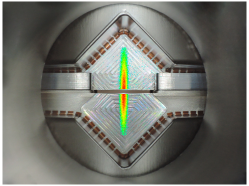

ALFA

Absolute Luminosity For ATLAS

ALFA Detectors

- Two stations at each ATLAS side, 240 m far from the IP1.
- Detectors move vertically ((y) direction) and take data $\sim$1 mm from the beam.
- 2×10 layers of scintillating fibres in pot – position measurement with precision of $\sim 30\ \mu$m.

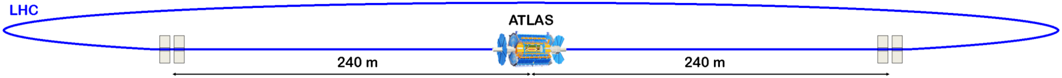

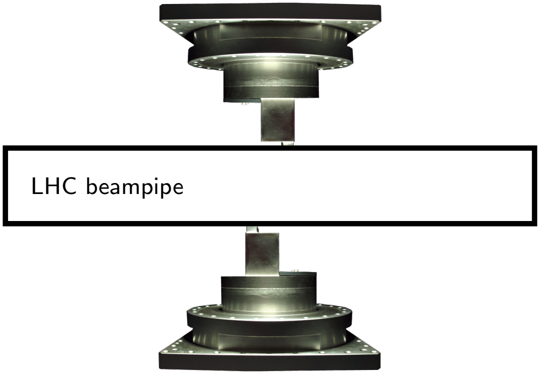

open

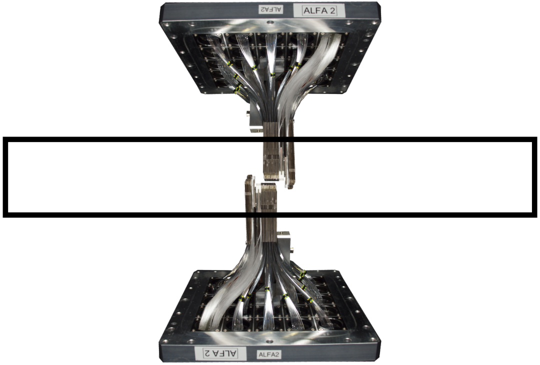

closed

ALFA Data-taking (2011 – 2023)

- Several dedicated, high-β^* campaigns in years 2011 – 2023.
- Initial programme of the elastic scattering measurement was extended to low-mass diffractive and exclusive measurements (addition of ATLAS "central" detector: APP B **42** (2011) 1861).
- Few results already published, more in the pipeline!

Year	β*	√s [TeV]	Comments
2011	90 m	7	elastics: NPB 889 (2014) excl. $\pi^+\pi^-$: EPJC 83 (2023) 627
2012	90 m	8	elastics: PLB 761 (2016) single diff.: JHEP 02 (2020) 042
2012	1 km	8	elastics dataset
2013	0.8 m	2.76	proton-lead dataset
2013	0.8 m	2.76	proton-proton reference dataset
2015	90	13	diffractive dataset
2016	2.5 km	13	elastics: EPJC 83 (2023) 441
2018	90 m	13	elastic (large *t*) and diff. datasets
2018	11 m	0.9	elastics (large *t*) dataset
2018	50/100m	0.9	elastics dataset
2023	3/6 km	13.6	elastics dataset

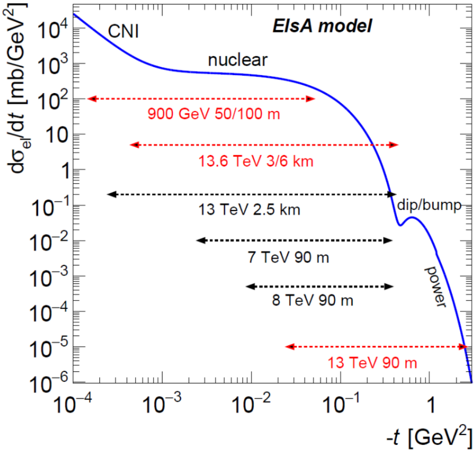

Elastic Scattering

Eur. Phys. J. C **83** (2023) 441

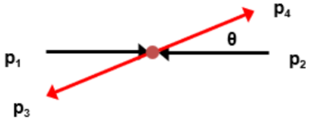

$$t = (p_1 - p_3)^2 = (p_2 - p_4)^2$$
$$t \approx -(p\theta)^2$$

pattern before selection:

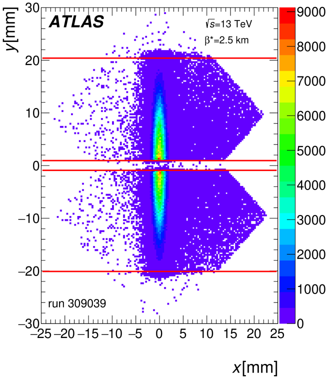

one of selection criteria: correlation between sides

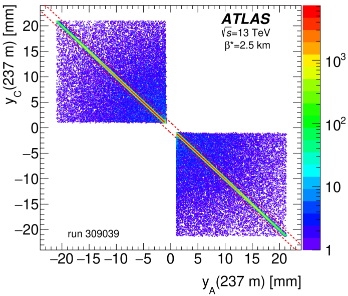

pattern after selection:

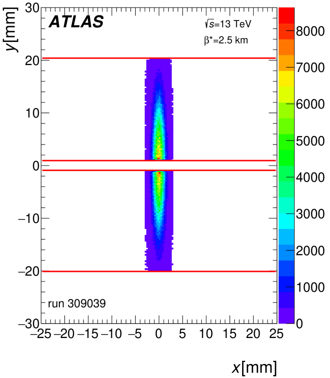

Selection criterion	Arm 1	Fraction	Arm 2	Fraction
Preselection	2 558 637			
Reconstructed tracks	1 289 282		1 269 355	
Cut on x A vs C (3.5σ)	1 254 738	97.32%	1 235 792	97.36%
Cut on y A vs C (2 mm)	1 249 888	96.95%	1 231 251	96.99%
Cut on x vs θ_x (3.5σ)	1 248 597	96.84%	1 230 084	96.91%
Beam-screen cut	1 243 941	96.48%	1 225 375	96.53%
Edge cut	1 231 848	95.55%	1 210 759	95.38%
Cut on y vs θ_y (40 µrad)	1 214 717	94.22%	1 195 251	94.16%
Total selected	2 409 968			

(Numbers of events)

Fill	Run	Luminosity [μb^{-1}]	Selected elastic event candidates	Reconstruction efficiency Arm 1 [%]	Reconstruction efficiency Arm 2 [%]
5313	308979	21.38	423 862	84.82 ± 0.56	83.11 ± 0.87
5313	308982	6.81	136 499	85.84 ± 0.54	84.44 ± 0.55
5314	309010	41.27	846 581	87.11 ± 0.51	85.00 ± 0.64
5317	309039	120.08	2 409 968	85.45 ± 0.49	83.23 ± 0.52
5317	309074	44.31	887 373	85.55 ± 0.39	83.48 ± 0.48
5321	309165	55.87	1 149 499	87.08 ± 0.40	85.41 ± 0.44
5321	309166	50.17	1 043 576	88.28 ± 0.38	86.43 ± 0.45
Total		339.89	6 897 358		

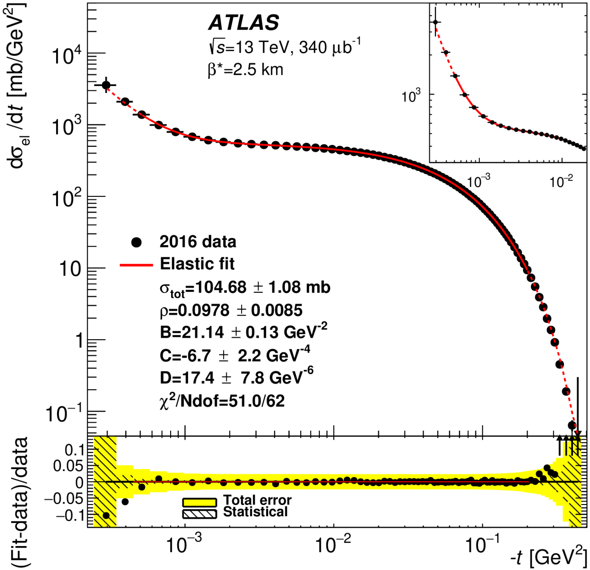

	σ_{tot} [mb]	ρ	B [GeV^{-2}]	C [GeV^{-4}]	D [GeV^{-6}]
Central value	104.68	0.0978	21.14	−6.7	17.4
Statistical error	0.22	0.0043	0.07	1.1	3.8
Experimental error	1.06	0.0073	0.11	1.9	6.8
Theoretical error	0.12	0.0064	0.01	0.04	0.15
Total error	1.09	0.0106	0.13	2.3	7.8

$\sqrt{s} = 13$ TeV, $L = 340\ \mu b^{-1}$

total cross-section:
$\sigma_{tot}(pp \to X) = 104.7 \pm 1.1$ mb

real-to-imaginary ratio of the nuclear elastic scattering: $\rho = 0.098 \pm 0.011$

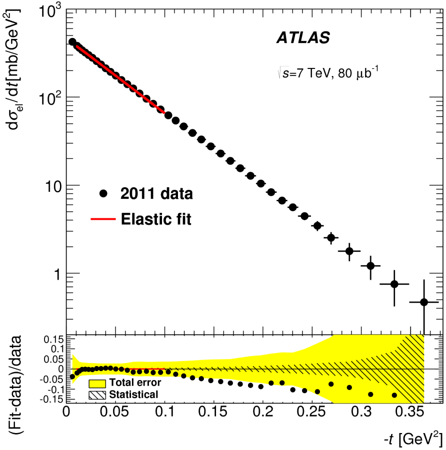

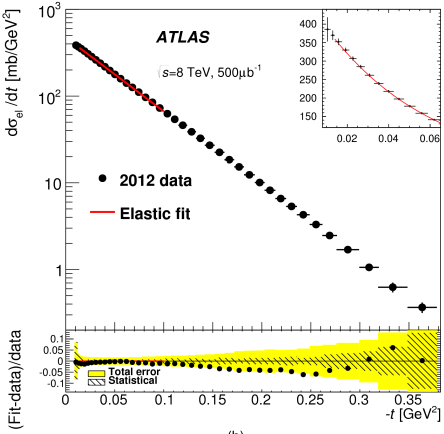

(b)

$\sqrt{s} = 7$ TeV, $L = 80\ \mu b^{-1}$
$\sigma_{tot}(pp \to X) = 95.35 \pm 0.38\ (stat.) \pm 1.25\ (exp.) \pm 0.37\ (extr.)$ mb
$B = 19.73 \pm 0.14\ (stat.) \pm 0.26\ (syst.)\ \mathrm{GeV}^{-2}$

$\sqrt{s} = 8$ TeV, $L = 500\ \mu b^{-1}$
$\sigma_{tot}(pp \to X) = 96.07 \pm 0.18\ (stat.) \pm 0.85\ (exp.) \pm 0.31\ (extr.)$ mb
$B = 19.74 \pm 0.05\ (stat.) \pm 0.23\ (syst.)\ \mathrm{GeV}^{-2}$

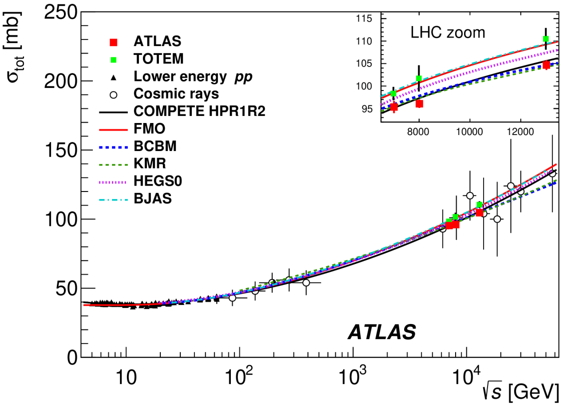

ATLAS
TOTEM
Lower energy pp
Cosmic rays
COMPETE HPR1R2
FMO
BCBM
KMR
HEGS0
BJAS
LHC zoom
ATLAS
σtot [mb]
√s [GeV]

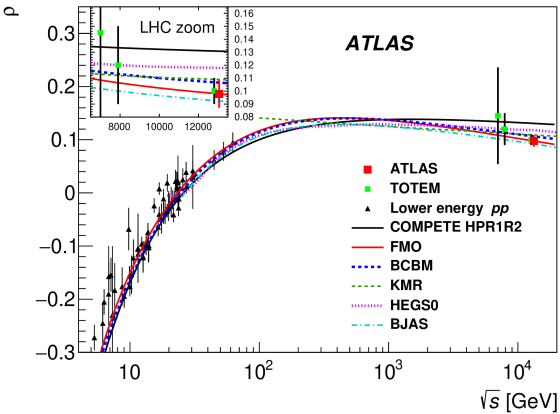

LHC zoom
ATLAS
ATLAS
TOTEM
Lower energy pp
COMPETE HPR1R2
FMO
BCBM
KMR
HEGS0
BJAS
ρ
√s [GeV]

Exclusive Pion Production

Eur. Phys. J. C **83** (2023) 627

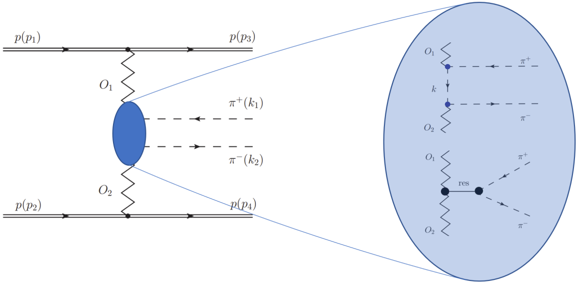

ALFA Exclusive Pion Analysis at $\sqrt{s} = 7$ TeV: Signal Selection

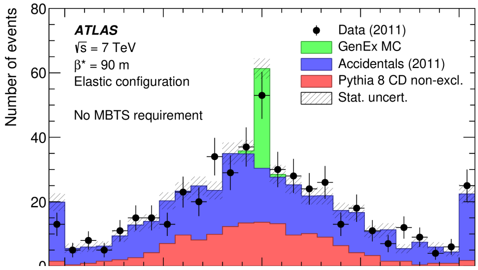

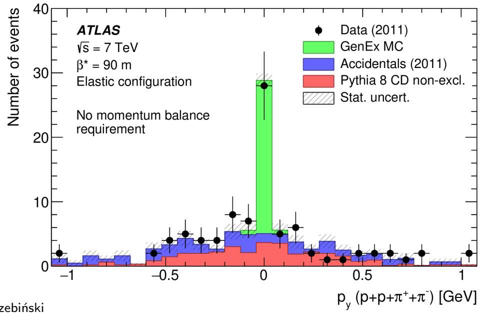

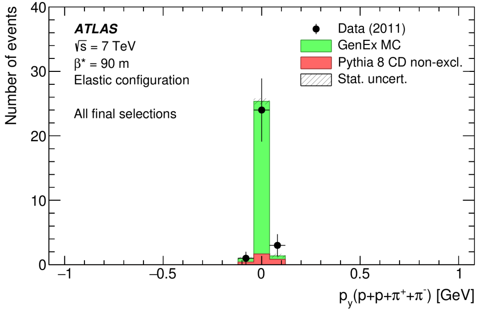

Selection	Configuration elastic	anti-elastic
Recorded ATLAS events	6 620 953	
Data quality and trigger preselections	1 106 855	397 683
ID selection (pion pair)	1 520	1 115
ALFA track selection (incl. clean track and uv-condition)	486	11
MBTS veto	136	5
ALFA geometry condition	96	5
Full system momentum balance in x and y	30	3
Fiducial region	28	3
(arm 0 + arm 1) **Total selected**	(18+10) **28**	(2+1) **3**

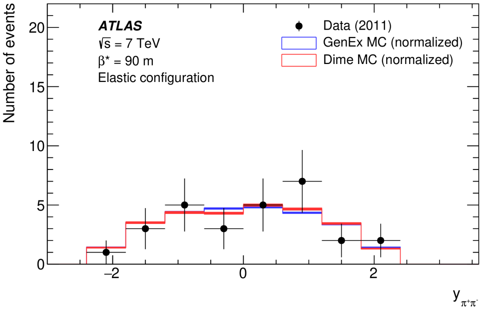

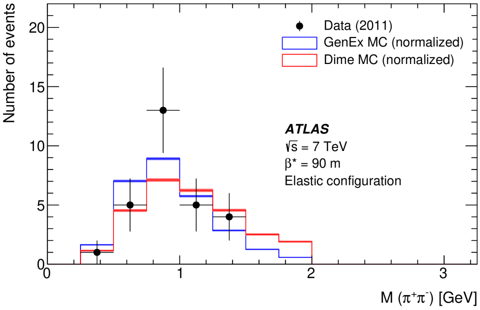

Exclusive $\pi^+\pi^-$ cross-section [µb]	
Elastic configuration	
Measurement	4.8 ± 1.0 (stat) $^{+0.3}_{-0.2}$ (syst) ± 0.1 (lumi) ± 0.1 (model)
GenEx $\times$ 0.22 (absorptive correction)	1.5
Dime	1.6
Anti-elastic configuration	
measurement	9 ± 6 (stat) $^{+1}_{-1}$ (syst) ± 1 (lumi) ± 1 (model)
GenEx $\times$ 0.22 (absorptive correction)	2
Dime	3

AFP

ATLAS Forward Proton

AFP: Silicon Trackers (SiT)

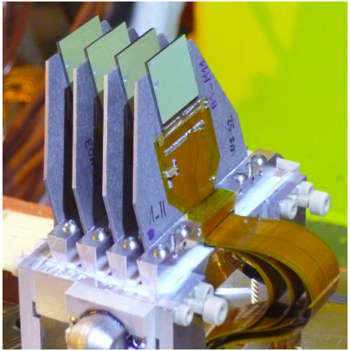

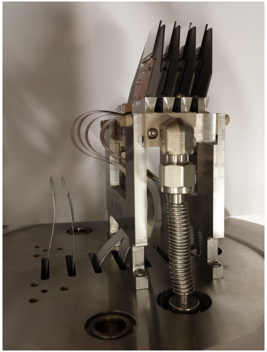

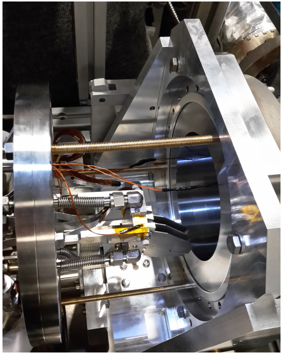

- Four detectors in each station.
- Technology: slim-edge 3D ATLAS IBL pixel sensors bonded with FE-I4 readout chips.
- Pixel size: 50x250 μm^2.
- Tilted by 14^0 to improve resolution in x.
- Resolution: $\sim$6 μm in x and $\sim$30 μm in y.
- Trigger: majority vote (2 out of 3; two chips in FAR station are paired and vote as one).

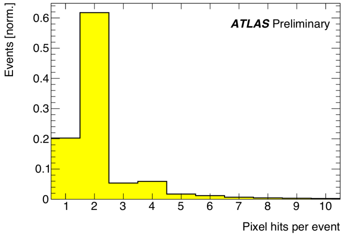

Proton Tagging or Position Measurement?

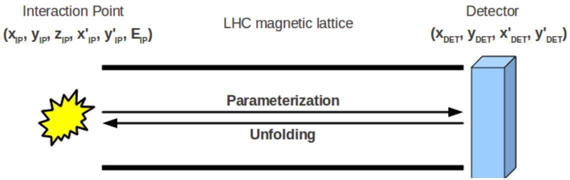

- At the interaction point proton (IP) is fully described by six variables: position (x_{IP}, y_{IP}, z_{IP}), angles (x'_{IP}, y'_{IP}) and energy (E_{IP}).
- They translate to unique position at the forward detector (x_{DET}, y_{DET}, x'_{DET}, y'_{DET}).
- Idea: get information about proton kinematics at the IP from their position in the AFP detector.
- Exclusivity: kinematics of scattered protons is strictly connected to kinematics of central system.
- Detector resolution play important role in precision of such method.

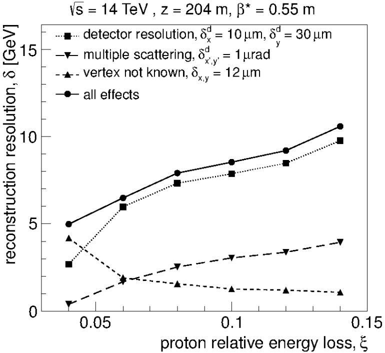

From ISRN High Energy Physics (2012) 491460; ATLAS-TDR-024

Data recorder so far:

- 32.0 fb^{-1} in Run 2,
- $34.1 + 26.3 + 108 = 168.4$ fb^{-1} in Run 3.
- In addition: few campaigns at low-μ.
- Note: not all of recorded data is useful for physics analyses.

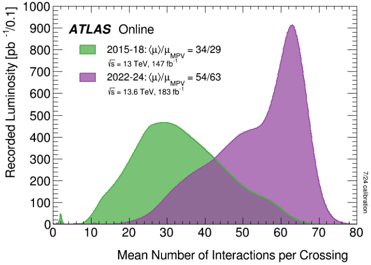

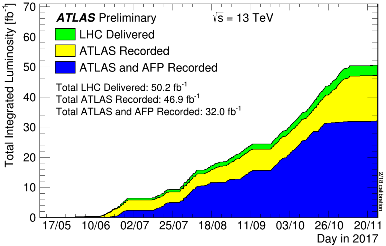

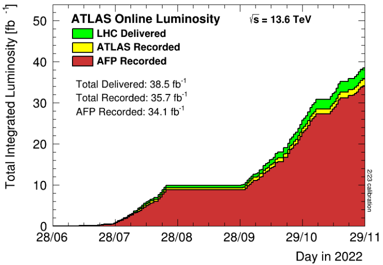

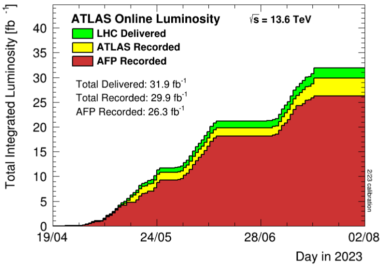

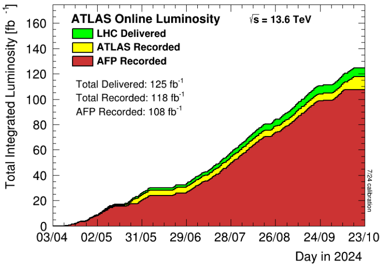

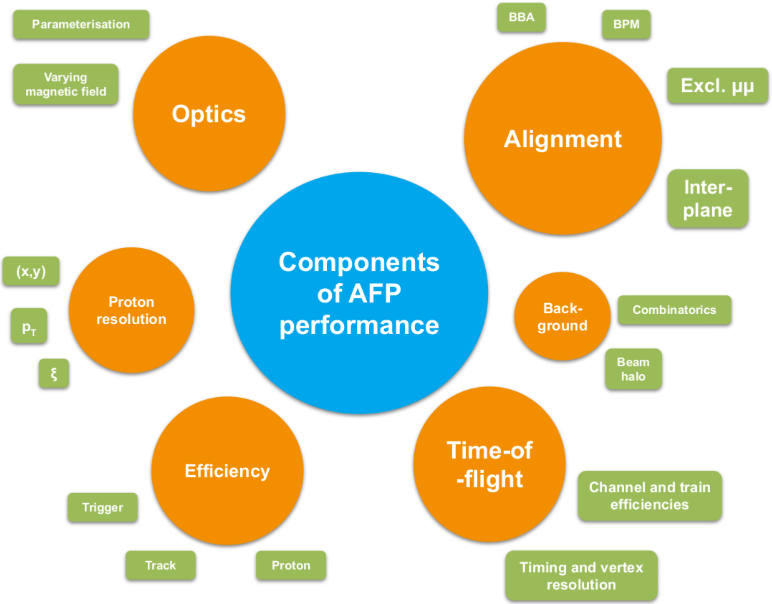
Parameterisation
Varying magnetic field
Optics
BBA
BPM
Alignment
Excl. μμ
Inter-plane
Components of AFP performance
(x,y)
p_T
ξ
Proton resolution
Back-ground
Combinatorics
Beam halo
Efficiency
Trigger
Track
Proton
Time-of -flight
Channel and train efficiencies
Timing and vertex resolution

Exclusive Di-lepton Production

Phys. Rev. Lett. **125** (2020) 261801

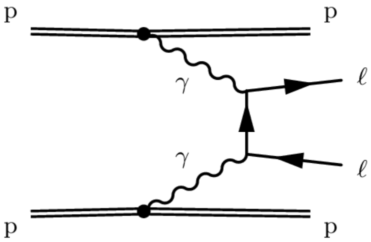

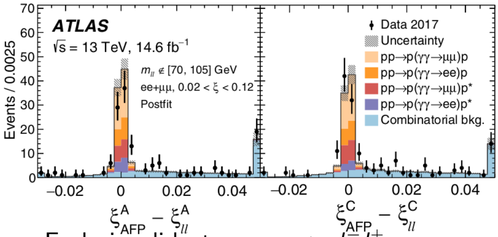

- Exclusive di-leptons, $pp \to pl^- l^+ p$:
  - proton(s) measured in AFP,
  - leptons ($\mu^+\mu^-$ or e^+e^-) measured in ATLAS.
- 2017 data; $\sqrt{s} = 13$; $L = 14.6$ fb^{-1}.
- Powerful background rejection due to AFP:
  - proton tagging,
  - kinematics match: proton vs lepton system.
- 57 (123) candidates in the $ee + p$ ($\mu\mu + p$) final state.
- Background-only hypothesis rejected with a significance exceeding 5σ in each channel.
- $\sigma_{ee+p} = 11.0 \pm 2.6(\mathrm{stat}) \pm 1.2(\mathrm{syst}) \pm 0.3(\mathrm{lumi})$,
  $\sigma_{\mu\mu+p} = 7.2 \pm 1.6(\mathrm{stat}) \pm 0.9(\mathrm{syst}) \pm 0.2(\mathrm{lumi})$.

Source of systematic uncertainty	Impact
Forward detector	
Global alignment	6%
Beam optics	5%
Resolution and kinematic matching	3–5%
Track reconstruction efficiency	3%
Alignment rotation	1%
Clustering and track-finding procedure	< 1%
Central detector	
Track veto efficiency	5%
Pileup modeling	2–3%
Muon scale and resolution	3%
Muon trigger, isolation, reconstruction efficiencies	1%
Electron trigger, isolation, reconstruction efficiencies	1%
Electron scale and resolution	1%
Background modeling	2%
Luminosity	2%

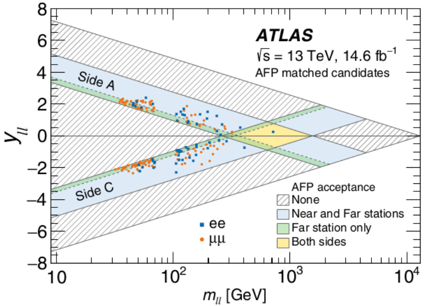

Search for Axion-like Particles

JHEP **07** (2023) 234

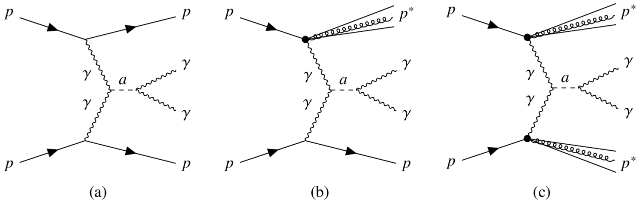

Search for Axion-like Particles

Selection	A-side	C-side
Preselection	69221	
$A_{\phi}^{\gamma\gamma} < 0.01$	7131	
$0.035 - \xi_{\mathrm{th}} < \xi_{\gamma\gamma} < 0.08 + \xi_{\mathrm{th}}$	2025	2075
$0.035 < \xi_{\mathrm{AFP}} < 0.08$	635	650
$\lvert\Delta\xi\rvert < \xi_{\mathrm{th}}$	219	222
Full selection	441	

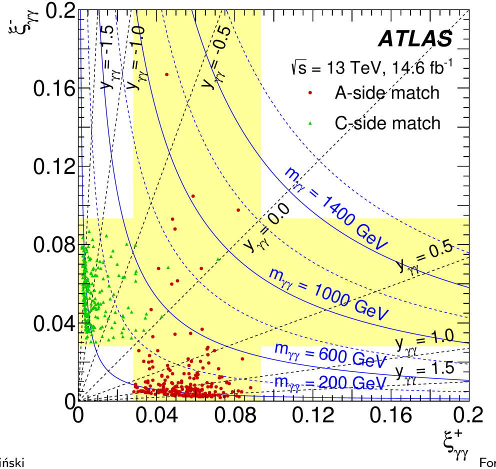

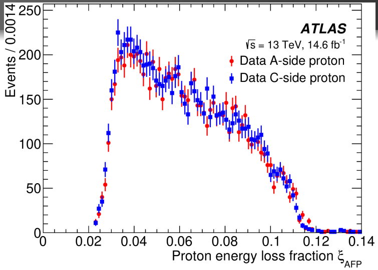

Source	Uncertainty
Signal yield uncertainty	
Pile-up reweighting	$^{+2.7}_{-2.6}$%
Luminosity	± 2.4%
Photon identification efficiency	$^{+1.6}_{-1.5}$%
Photon isolation efficiency	± 1.9%
Beam optics between ATLAS central and AFP detectors	$^{+0.8}_{-3.4}$%
AFP global alignment	$^{+10.0}_{-8.6}$%
Proton reconstruction efficiency	$^{+3.0}_{-2.2}$%
Showering in the AFP	$^{+0.0}_{-6.6}$%
Background modelling (mass-dependent)	$\pm$(0.02–0.7) events
Signal modelling	
Photon energy resolution	$^{+14.1}_{-4.8}$%
Photon energy scale	$\pm$(0.5–1.0)%
Signal cross-section uncertainty	
Soft survival factor (exclusive process)	± 2%
Soft survival factor (single-dissociative process)	± 10%
Soft survival factor (double-dissociative process)	± 50%

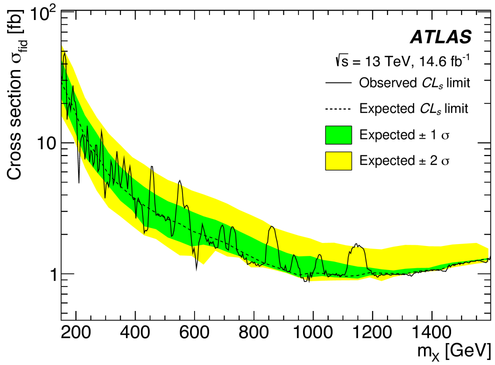

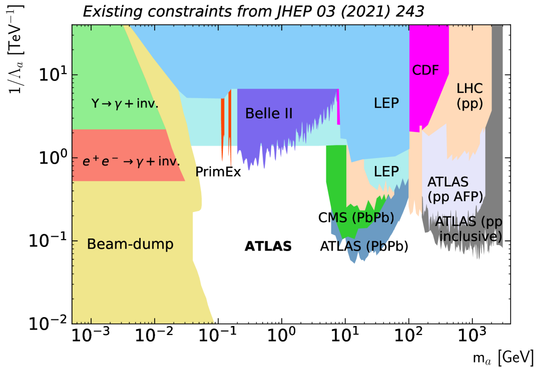

- Dominant background contribution – pair of photons overlaid with pile-up proton – was estimated using "mixed events" technique smoothed by the functional decomposition method.
- After analysing 14.6 fb^{-1} of data collected at 13 TeV, 441 candidate signal events were selected.
- Search for a narrow resonance in the diphoton mass distribution in the range 150–1600 GeV shown no excess above the smooth background.
- This resulted in setting the upper limits on the production cross section of a narrow resonance – corresponding to an axion-like particle (ALP) – being set.

Summary

- Forward proton detectors enhance the ATLAS physics programme, so far published results of:
  - elastic analyses (total cross section, nuclear slope, ρ parameter) with ALFA,
  - exclusive pion production with ALFA,
  - exclusive lepton production with AFP,
  - search for a new physics with AFP.
- **Huge efforts of many to have system operational and in a good shape!**
- ALFA concluded its programme in 2023, after 12 years of data-taking.
- AFP continues to take data in regular and special runs:
  - 2 results using Run 2 data already published, few more analyses at $\sqrt{s} = 13$ TeV ongoing,
  - performance work on Run 3 data-set in progress $\rightarrow$ significant increase of statistics wrt. Run 2 is expected.
- With data already recorded on tape, ATLAS forward proton detectors will continue delivering interesting physics results in the coming years!

The work of MT was partially supported by Polish National Science Centre (project no. UMO-2019/34/E/ST2/00393).

Backup

expected t-acceptance:

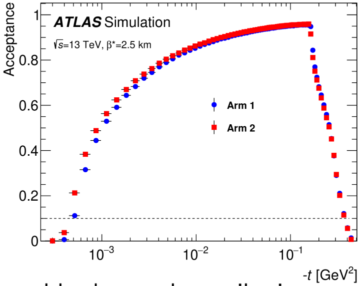

uncertainties of t-reconstruction methods:

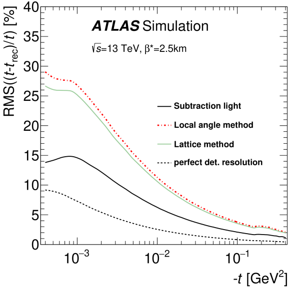

expected background contribution:

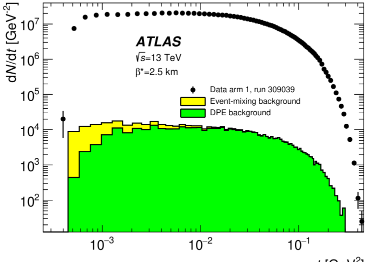

t-value migration matrix:

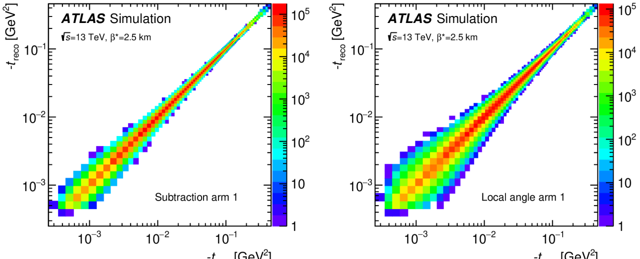

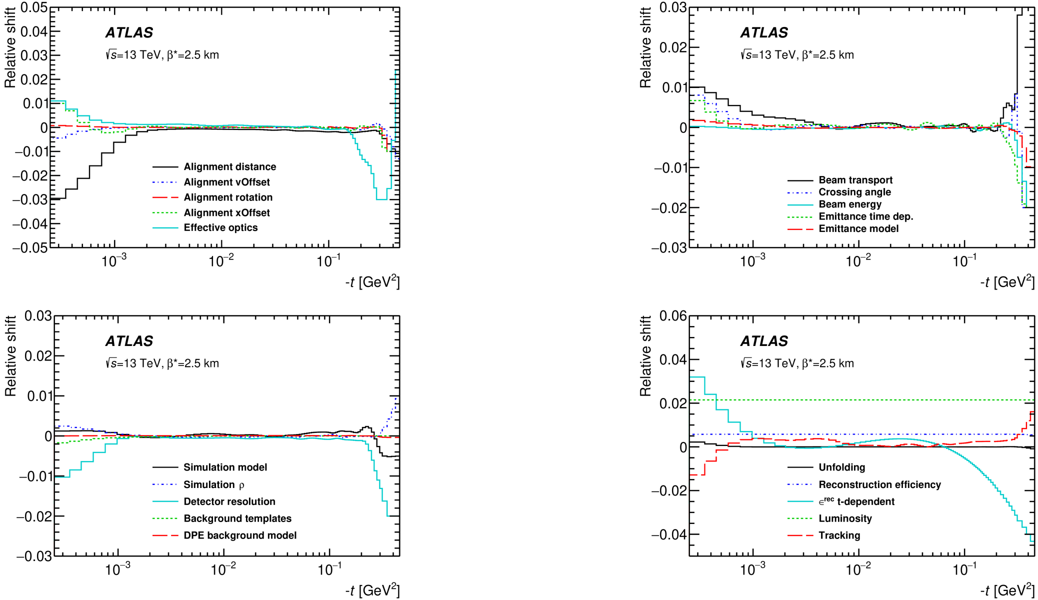
ATLAS
√s=13 TeV, β*=2.5 km
Relative shift
-t [GeV²]
Alignment distance
Alignment vOffset
Alignment rotation
Alignment xOffset
Effective optics
Beam transport
Crossing angle
Beam energy
Emittance time dep.
Emittance model
Simulation model
Simulation ρ
Detector resolution
Background templates
DPE background model
Unfolding
Reconstruction efficiency
ε^rec t-dependent
Luminosity
Tracking

Pile-up – multiple collisions during one bunch crossing (mostly min-bias).

signal

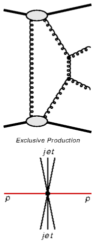

background

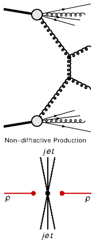

background

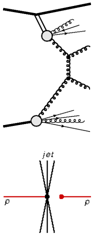

Idea:

- measure difference of time of flight of scattered protons, $(t_A - t_C)/2$
- compare to vertex reconstructed by ATLAS, $(t_A - t_C) \cdot c/2 - z_{ATLAS}$

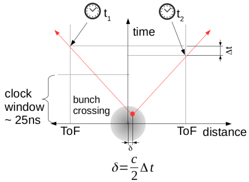

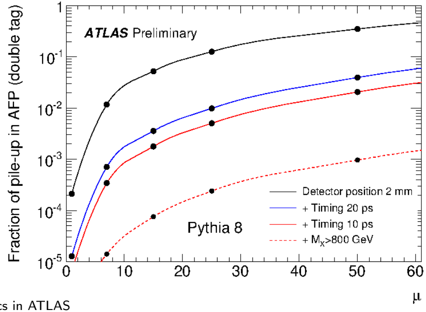

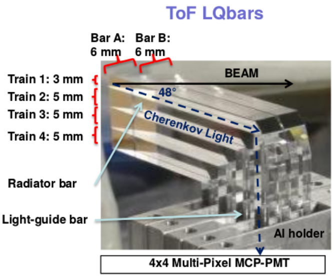

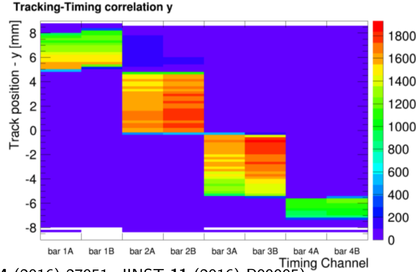

Setup and performance shown above are from test-beam (Opt. Express **24** (2016) 27951, JINST **11** (2016) P09005).

- 4x4 quartz bars oriented at the Cherenkov angle with respect to the beam trajectory.
- Light is directed to Photonis MCP-PMT.
- Expected resolution: ∼25 ps.
- Installed in both FAR stations.

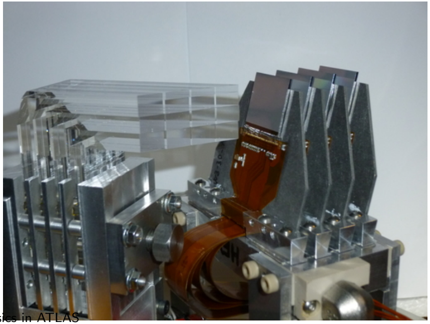

Performance: Time-of-Flight

- Performance analysis based on 2017 data (taken with $\mu \approx 2$): ATL-FWD-PUB-2021-002.
- Poor efficiency of few percent due to fast PMT degradation; effect not expected during Run 3 due to new PMTs.
- Very good timing resolution: 20 – 50 ps for single bar.
- Overall time resolution of each ToF detector:
  - 20 ± 4 ps for side A,
  - 26 ± 5 ps for side C,
  - note: systematic uncertainties dominate.

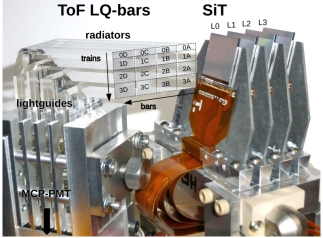

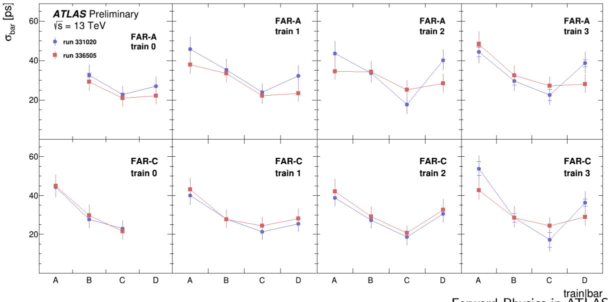

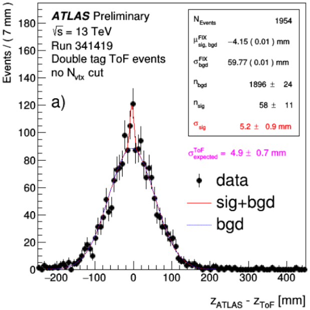

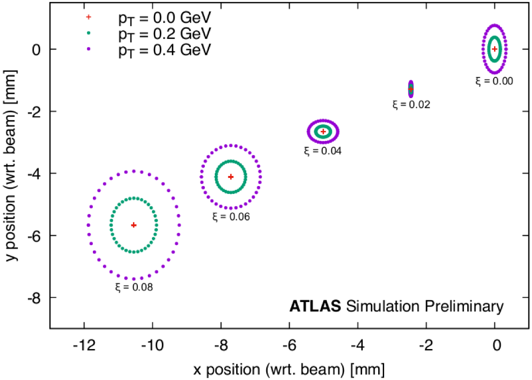

p_T = 0.0 GeV
p_T = 0.2 GeV
p_T = 0.4 GeV
ξ = 0.00
ξ = 0.02
ξ = 0.04
ξ = 0.06
ξ = 0.08
ATLAS Simulation Preliminary
y position (wrt. beam) [mm]
x position (wrt. beam) [mm]

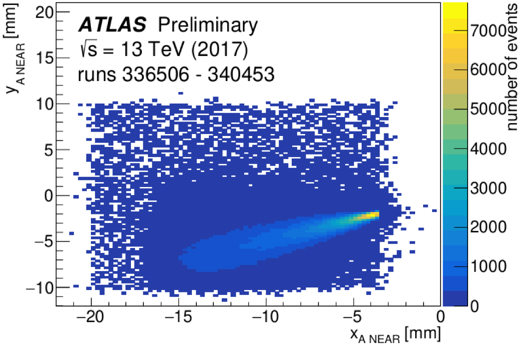

ATLAS Preliminary
$\sqrt{s}$ = 13 TeV (2017)
runs 336506 - 340453
$y_{A\,NEAR}$ [mm]
$x_{A\,NEAR}$ [mm]
number of events

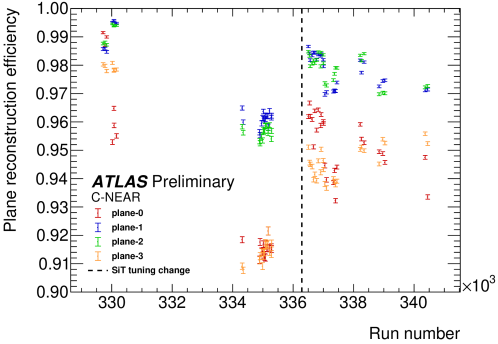
ATLAS Preliminary
C-NEAR
plane-0
plane-1
plane-2
plane-3
SiT tuning change
Plane reconstruction efficiency
Run number
$\times 10^3$

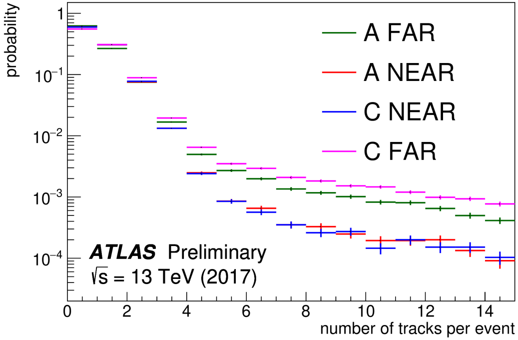
A FAR
A NEAR
C NEAR
C FAR
ATLAS Preliminary
$\sqrt{s}$ = 13 TeV (2017)
probability
number of tracks per event

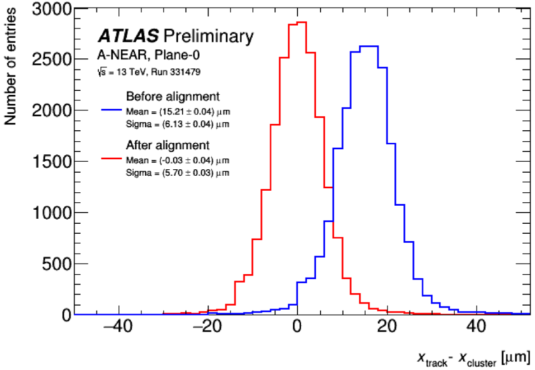
ATLAS Preliminary
A-NEAR, Plane-0
√s = 13 TeV, Run 331479
Before alignment
Mean = (15.21 ± 0.04) µm
Sigma = (6.13 ± 0.04) µm
After alignment
Mean = (-0.03 ± 0.04) µm
Sigma = (5.70 ± 0.03) µm
Number of entries
x_track - x_cluster [µm]

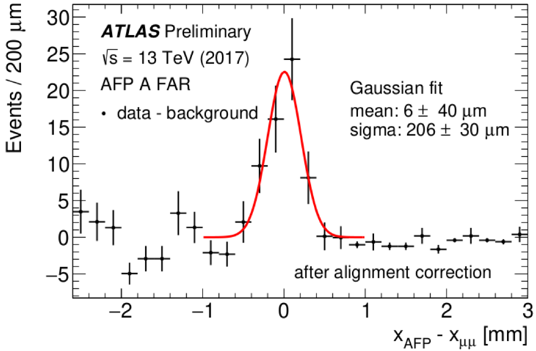
ATLAS Preliminary
√s = 13 TeV (2017)
AFP A FAR
• data - background
Gaussian fit
mean: 6 ± 40 µm
sigma: 206 ± 30 µm
after alignment correction
Events / 200 µm
x_AFP - x_µµ [mm]

AFP Performance: Acceptance